UDC 631.6.02:[(292):485+438.42(477)
DOI: https://doi.org//10.31073/abg.68.04

SPATIAL AND TEMPORAL DYNAMICS OF RAINFALL EROSIVITY FACTOR IN POLISSYA AND FOREST-STEPPE OF UKRAINE

YU. A. NYKYTIUK[1], O. I. KRAVCHENKO[2]
[1]Polissia National University (Zhytomyr, Ukraine)
[2]Institute of Animal Breeding and Genetics nd. a. M. V. Zubets of NAAS (Chubynske, Ukraine)
https://orcid.org/0000-0001-9142-7699 – YU. A. Nykytiuk
https://orcid.org/0009-0002-5468-4404 – O. I. Kravchenko
kravchenko.irgt@gmail.com

The article presents the results of research on the study of spatial and temporal variability of the precipitation erosion factor in the period from 1960 to 2023 within the administrative regions of Polissya and Forest-Steppe of Ukraine. MEM-spatial variables were able to explain 80.8% of the variability of the precipitation erosion factor. The ANOVA revealed that 8 canonical axes, which were extracted after the RDA analysis, were statistically significant. The canonical axes represent different spatial patterns of variability of the precipitation erosion factor. The contribution of spatial MEM variables to the explanation of the canonical axes is different, which allows us to identify the hierarchical structure of variability of the main spatial patterns of precipitation in the region. The canonical axes denoting the main spatial patterns of precipitation erosion variability were correlated with soil properties and land cover types. The temporal AEM predictors 4, 17, 25, 29, 32, 39, 44, and 61 were able to statistically significantly predict temporal patterns of precipitation variability within the study area. These temporal predictors were able to explain 25.9% of the variation in the total matrix of precipitation erosion coefficients. The highest explanatory power of the AEM predictors was found for the southern and southeastern regions, and the lowest for the western regions. The forecast for administrative regions was made for the period up to 2060. The spatial and temporal dynamics of the precipitation erosion factor has a complex hierarchical structure, which can be represented as a set of spatial and temporal patterns with a specific ratio of components of different scale levels. In the spatial context, the patterns are a superposition of processes of broad-, medium-, and detailed-scale levels. The combination of these levels, the nature of spatial variability, and the correlation with soil and landscape indicators allows us to formulate hypotheses about the relevant processes that generate spatial patterns of precipitation erosion factors. Obviously, there are three groups of factors that cause natural variability in precipitation erosion. The first group includes factors of geographical nature, the second includes factors caused by soil cover heterogeneity, and the third includes factors caused by landscape cover heterogeneity. The latter also includes factors that are the result of anthropogenic transformation of landscapes, primarily through agricultural activities. The factors of geographical origin are represented by large-scale patterns, soil factors are represented mainly by medium-scale patterns and to some extent by detailed-scale patterns, and landscape factors are represented mainly by detailed-scale patterns and to a lesser extent by medium-scale patterns.

Keywords: **climate change, spatial patterns, temporal variability, landscape, land cover, soil erosion**

ПРОСТОРОВО-ЧАСОВА ДИНАМІКА ФАКТОРУ ЕРОЗИВНОСТІ ОПАДІВ У ПОЛІССІ ТА ЛІСОСТЕПУ УКРАЇНИ

Ю. А. Никитюк[1], О. І. Кравченко[2]
[1]Поліський національний університет (Житомир, Україна)
[2]Інститут розведення та генетики тварин імені В.М. Зубця НААН (Чубинське, Україна)

У статті наведено результати досліджень щодо вивчення просторової та часової мінливості фактору ерозії опадів у період з 1960 по 2023 роки у межах адміністративних районів Полісся та Лісостепу України. MEM-просторові змінні були здатні пояснити 80,8% мінливості коефіцієнту ерозивності опадів. ANOVA дозволила встановити, що статистично вірогідними є 8 канонічних осей, які були екстраговані після RDA-аналізу. Канонічні осі представляють різні просторові патерни мінливості фактору ерозивності опадів. Внесок просторових MEM-змінних у пояснення канонічних осей є різним, що дозволяє виявити ієрархічну структуру мінливості головних просторових патернів опадів у регіоні. Канонічні осі які позначають головні просторові патерни мінливості ерозивності опадів корелювали з ґрунтовими властивостями та типами ландшафтного покриву. Часові AEM-предиктори 4, 17, 25, 29, 32, 39, 44 та 61 були здатні статистично вірогідно часові патерни мінливості опадів у межах дослідженої території. Ці часові предиктори були здатні пояснити 25,9% варіювання тотальної матриці коефіцієнтів ерозивності опадів. Найбільша пояснювальна здатність AEM-предикторів була встановлена для південних та південно-східних районів, а найменша – для західних. Прогноз по адміністративних районах був зроблений на період до 2060 року. Просторово-часова динаміка фактору ерозивності опадів має складну ієрархічну структуру, яка може бути представлена як сукупність просторових та часових патернів зі специфічним співвідношенням складових різного масштабного рівня. У просторовому контексті, патерни представляють собою суперпозицію процесів широко-, середньо- та детально-масштабного рівнів. Комбінація цих рівнів, характер просторової мінливості та кореляція з ґрунтовими та ландшафтними показниками дозволяє сформулювати гіпотези про відповідні процеси, які генерують просторові патерни фактори ерозивності опадів. Очевидно, що існує три групи факторів, які викликають закономірну мінливість ерозивності опадів. До першої групи належать фактори географічної природи, до другої належать фактори, які викликані неоднорідністю ґрунтового покриву, а до третьої належать фактори, які викликані неоднорідністю ландшафтного покриву. До останнього належать також фактори які є наслідком антропогенного перетворення ландшафтів, у першу чергу через сільськогосподарську діяльність. Фактори географічного походження представлені широкомасштабними патернами, ґрунтові фактори представлені переважно середньомасштабними патернами та певною мірою – детально масштабними, а ландшафтні фактори представлені переважно детально-масштабними патернами та меншою мірою – середньо-масштабними патернами.

Ключові слова: **кліматичні зміни, просторові патерни, часова мінливість, ландшафт, ґрунтовий покрив, ерозія ґрунту**

Problem definition. The phenomenon of water erosion represents a significant threat to the sustainability of agricultural production. Soil erosion can be defined as the detachment and transport of soil particles by erosive agents, most commonly water and/or wind. It is a natural process, but human activities, such as agriculture, forestry, mining, and construction, can disrupt or destroy vegetation, loosen soil, and significantly increase the risk of soil erosion losses during subsequent rains, runoff, or storms. The study of spatial and temporal variability of the precipitation erosion factor is an important problem for solving the problems of agroecological zoning of territories and predicting the variability of erosion processes in the context of global climate change.

Analysis of recent research and publications. A substantial body of evidence indicates that climate change will exacerbate the severity of soil erosion in a range of geographical areas (Brannigan et al., 2022). Soil erosion results in soil degradation and impairs soil functions, including filtration, nutrient cycling, water retention, and soil organic matter composition (Telo da Gama , 2023). It should be noted that erosion causes numerous adverse effects on people and the environment beyond agricultural land (Horrigan et al., 2002) and poses a serious threat to the sustainable use of soil in Europe (Panagos, 2015). The impact of climate change on rainfall erosion activity and the increased risk that these changes may pose to soil erosion processes necessitates an understanding of

the dynamics of these processes in space and time. As a consequence of an increase in the frequency of extreme precipitation events, there has been an increase in rainfall erosion in recent years (Diodato, 2017). An increase in climatic variability, including intense precipitation, also has an aggravating effect on soil and intensifies erosion processes (Burt et al., 2016) It is thus imperative to ensure the continual updating of information pertaining to the factors that regulate erosion processes, with a view to guaranteeing optimal agricultural management and the implementation of preventive measures in areas characterised by an elevated risk of erosion. It is imperative to develop a reasonable forecast of erosion changes in the coming decades in order to facilitate effective land management and the conservation of ecosystems. This is particularly crucial given the general expectation of increased precipitation intensity in the context of global warming (Biasutti et al., 2015) which is why assessing the risk of soil loss and its spatial distribution is one of the key factors for successful erosion assessment (Parveen et al., 2019). As soil erosion is difficult to measure at large scales, soil erosion models are important assessment tools at regional, national, and European levels (Parveen et al., 2019, Zymaroieva et ai., 2021). Soil erosion prediction models are effective tools to help guide and inform soil protection planning and practice (Yin et al., 2015). These models encompass a multitude of analogous and disparate elements, yet they are unified by a common denominator: the rainfall erosion factor (R). This factor serves to quantify the potential for rainfall to precipitate soil loss from slopes, and it is regarded as one of the most pivotal elements in the estimation of soil erosion. Of all the erosion factors, rainfall erosion and factors pertaining to land cover and land use types are regarded as the most dynamic (Panagos et al., 2016). Climate change can lead to changes in rainfall characteristics and is thus a major challenge for soil conservation (Meusburger et al., 2012). Nevertheless, the RUSLE methodology necessitates the utilisation of precise precipitation data and the accurate computation of each storm erosion index to ascertain an average long-term rainfall erosion rate. This process is inherently arduous (Diodato et al., 2006).

Natural complexes are complex systems comprising a multitude of interacting objects across a range of spatial and temporal scales. The characterisation of these scales represents a crucial step in the comprehension and prediction of the consequences of alterations in the processes that regulate these systems. It employs mathematical and statistical techniques that permit the quantification of spatial and temporal complexity and are sufficiently robust to accommodate any type of sampling design. The spatial patterns of natural phenomena can be attributed to a multitude of endogenous and exogenous processes occurring at varying spatial scales (Vaclavik et al., 2012). The analysis of combinations of processes and scales necessitates the utilisation of mathematical tools that are capable of accounting for or modelling large-scale ordered patterns (Dray et al., 2012). Among the statistical methods, the most suitable for analysing such patterns are Moran's eigenvector maps (MEMs) (Dray et al., 2006) and their original form, neighbourhood principal coordinate matrices (Borcard et al., 2002). MEMs are derived from the theory of spectral graphs and are capable of characterising a wide range of autocorrelation structures based on the study design, specifically the distances between sample points or time (Dray et al., 2006). In other words, it is a spectral decomposition of the spatial (or temporal) relationships between sample points (or dates). The aforementioned decomposition generates eigenfunctions, which are novel orthogonal variables that can be employed in statistical models as explanatory variables representing the spatial or temporal relationships between the study sites (Brind`Amour et al., 2018).

Task definition. The modelling of R-factor variability over time is primarily concerned with the identification of a time trend, whereas the modelling of time variability is focused on the spatial interpolation of this indicator (Ma et al., 2014). The issue of the hierarchical organisation of the spatial and temporal variability of the R-factor is not even addressed. In light of the aforementioned shortcomings, the present study aims to elucidate the hierarchical structure of spatial and temporal variability of the R-factor within the Polissya and Forest-Steppe regions of Ukraine.

Methods of research. This study investigates the spatial and temporal variability of the precipitation erosion factor (R-factor) within ten administrative regions of the north and northwest of Ukraine. The region encompasses both the Polissya and Forest-Steppe geographical zones. Prior to

the 2015–2022 reform of Ukraine's administrative and territorial structure, the environmental characteristics were averaged within the administrative regions. This is due to the fact that the area of the traditional rayons is smaller and more ecologically homogeneous than that of the new administrative units.

The RUSLE model was employed for the estimation of annual soil loss. The RUSLE model was developed with the objective of predicting long-term average annual soil loss. The RUSLE equation is used to calculate the average annual erosion expected on field slopes (Wischmeier et al., 1978):

$$A = R + K + LS + C + P,$$

where the term "A" represents the calculated spatial average soil loss and average temporal soil loss per unit area, expressed in the units selected for "K" and for the specified period designated for "R." In practice, the units chosen for A are typically tons per hectare per year (t ha^{-1}/year), for R it is the precipitation-runoff erosion factor, which is the precipitation erosion rate plus a factor for any significant runoff from snowmelt, expressed in MJ mm ha^{-1} h^{-1} per year, and for K it is the soil erosion factor, which is the soil loss factor per unit of erosion index for a given soil measured on a standard plot, defined as a 22. The slope length factor (L) is defined as the ratio of soil loss from the length of the field slope to the soil loss from a standard plot measuring 22 m^2. In this example, the slope length is 1 m, the slope gradient is 9%, and the soil loss is expressed in t ha^{-1} MJ mm^{-1}. A one-metre-long slope under identical conditions; S is the slope steepness factor, representing the ratio of soil loss from the field slope gradient to soil loss from a 9% slope under otherwise identical conditions; C is the cover management factor, representing the ratio of soil loss from an area with a given cover and management to soil loss from an identical area under cultivated continuous break; P is the practical support factor, representing the ratio of soil loss with support such as contouring, strip mowing or terracing to soil loss under straight farming up and down the slope. The L and S factors represent the non-dimensional effects of slope length and steepness, respectively, whereas the C and P factors represent the non-dimensional effects of cropping and management systems, as well as erosion control practices. In general, the parameters of the RUSLE equation were classified into three categories: erosivity, erosion sensitivity, and management factors. All of the aforementioned parameters were determined based on geomorphic and precipitation characteristics (Zerihun et al., 2018).

In the present study, precipitation data for a period of 64 years (1960–2023) were employed to calculate the rainfall erosivity factor (R-factor) using the following equation (Wischmeier et al., 1978):

$$R = \sum_{i=1}^{12} 1.735 \times 10^{\left(1.5 log_{10}\left(\frac{P_i^2}{P}\right) - 0.08188\right)}$$

where R is the rainfall erosivity factor (MJ mm ha^{-1} h^{-1} per year); R_i is monthly precipitation (mm); P is annual precipitation, mm.

The functions provided by the *adespatial* package (Dray et al., 2018) were employed for the multiscale analysis of spatial and temporal multidimensional data. The spatial neighborhoods between points whose coordinates correspond to the centroids of administrative districts are managed in objects of the spdep class with the designation "*nb*". The objects of this class correspond to the concept of connectivity matrices and can be represented by an unweighted graph. A variety of functions are available for the creation of nb objects from geographic coordinates of sites. The adespatial package provides a range of tools for the construction of spatial predictors that can be incorporated into multivariate analysis. Moran eigenvector maps (MEMs) offer the most flexible structure for the modelling of spatial and temporal patterns.

WorldClim 2, based on a dataset of spatially interpolated monthly climate data for global land areas with a very high spatial resolution (approximately 1 km^2), was used as a spatial sample of precipitation in the study area (Cedrez et al., 2018, Fick et al., 2017). WorldClim 2 raster models were generated for the period 1960–2023. Data on the spatial variability of soil cover in the region

were obtained from the Harmonized World Soil Database (Version 2.0) (Aksoy et al., 2023). The soil properties were obtained from the SoilGRIDS database (www.isric.org/explore/soilgrids) using the *geodata* package (Hijmans et al., 2024). Information on landscape cover types was obtained from the GlobCover database land Cover Maps (GlobCover) (https://due.esrin.esa.int/page_globcover.php). Descriptive statistics were calculated in StatSoft 12.0.

Presentation of the main research findings

Spatial variation of the rainfall erosivity coefficient

The rainfall erosivity coefficient ranged from 179.9 ± 114.7 (in 2015) to 616.0 ± 468.9 (in 1974) MJ mm ha^{-1} h^{-1} per year. The MEM-spatial variables were able to explain 80.8% of the variability in the precipitation erosion coefficient ($F = 11.4$, $P < 0.001$). The ANOVA revealed that 8 canonical axes that were extracted after the RDA analysis were statistically significant (Fig. 1).

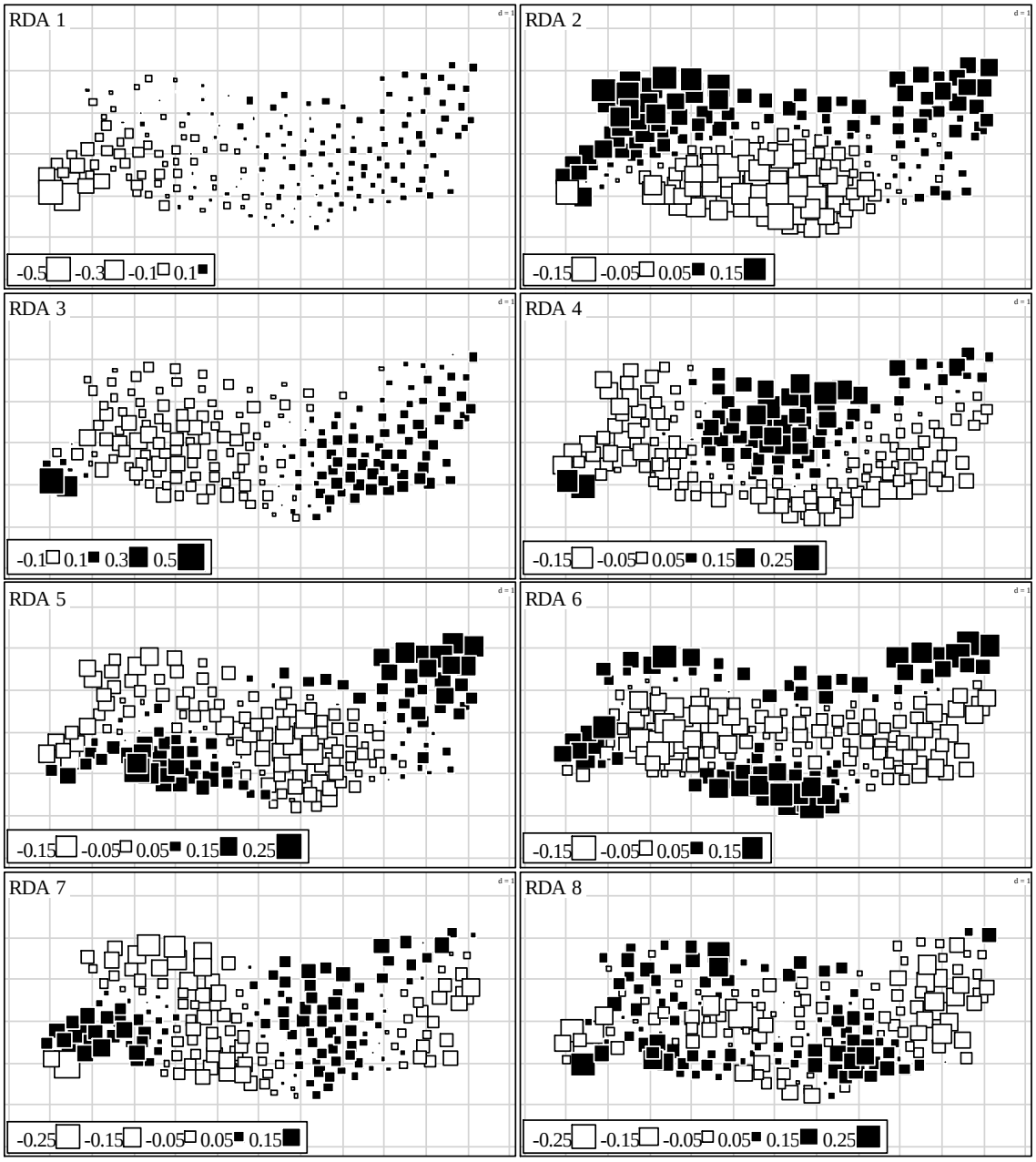

Fig. 1. **Spatial variability of the canonical axes selected after conditional redundancy analysis with spatial MEM variables as predictors: RDA1 explains 50.7% of the variation in the precipitation erosion coefficient (*F* = 211.4, *P* < 0.001), RDA2 explains 14.6% of the variation in the precipitation erosion coefficient (*F* = 35.9, *P* < 0. 001), RDA3 explains 14.1% of the variation in the precipitation erosion coefficient (*F* = 34.7, *P* < 0.001), RDA4 explains 6.0% of the variation in the precipitation erosion coefficient (*F* = 13.9, *P* < 0. 001), RDA5 explains 2.8% of**

the variation in the precipitation erosion coefficient (F = 7.0, P = 0.002), RDA6 explains 1.4% of the variation in the precipitation erosion coefficient (F = 3.9, P = 0. 006), RDA7 explains 1.1% of the variation in the precipitation erosion coefficient (F = 3.2, P = 0.03), RDA8 explains 0.7% of the variation in the precipitation erosion coefficient (F = 2.5, P = 0.05)

The canonical axes represent different spatial patterns of variability of the precipitation erosion factor. The RDA1 axis differentiates the plain part of the region from the foothill part. The RDA2 axis indicates differences in the dynamics of erosion processes in the north, east, and west of the region, on the one hand, and in the center and south of the region, on the other. Axis RDA3 draws attention to the spatial pattern when the dynamics of the precipitation erosion factor in the east and west coincide and are opposite to the rhythm of the process in the rest of the territory. Axis RDA4 indicates synchronized patterns of the precipitation erosion factor in the west, northeast, and center in the north, which are opposed to the dynamics in other parts of the region. Axis RDA5 contrasts the dynamics of erosion processes in the northeast and southwest on the one hand and the rest of the region on the other. The RDA6 axis distinguishes the dynamics in the north and south of the region from those in its central part. The RDA7 and RDA8 axes indicate the presence of complex detailed–scale patterns of variability in the precipitation erosion factor.

The contribution of spatial MEM variables to the explanation of the canonical axes is different, which allows us to identify the hierarchical structure of variability of the main spatial precipitation patterns in the region (Fig. 2). The RDA1 and RDA2 axes represent the large–scale component of precipitation variability. In the RDA1 variation, the large–scale component is predominant. RDA1 indicates the differentiation of patterns of the precipitation erosion coefficient in the meridional direction with the allocation of the eastern and western sectors of the region. RDA1 demonstrates autocorrelation in time with a lag of 5 years (r = –0.19, P = 0.05). RDA2 differentiates the region into northern, eastern, and western sectors and central and southern sectors. RDA2 shows autocorrelation in time with a lag of 3 years (r = –0.22, P = 0.03). The variation of the RDA3 axis is dominated by large– and small–scale spatial components. This axis differentiates the dynamics of the precipitation erosion coefficient of the eastern and extreme western (foothill) parts of the region, on the one hand, and the other part of the region, respectively. RDA3 demonstrates autocorrelation in time with a lag of 8 years (r = –0.15, P = 0.05).

The variation of the RDA4 axis includes large–, medium–, and detailed–scale spatial components, but the medium–scale component predominates. This axis differentiates between the dynamics of precipitation erosion in the northern, central, and far western parts of the region on the one hand and in the other part of the region. RDA4 demonstrates autocorrelation in time with a lag of 1 year (r = +0.13, P = 0.05). The variation of the RDA5 axis is dominated by large– and medium–scale spatial components. This axis differentiates precipitation dynamics in the eastern and southwestern parts on the one hand and in the western part and diagonal from northwest to southeast on the other hand. RDA5 shows autocorrelation in time with a lag of 1 year (r = –0.38, P < 0.01) and a lag of 2 years (r = +0.35, P < 0.01). The variation of the RDA6 axis represents the large–, medium–, and detailed–scale spatial components. This axis differentiates the dynamics of precipitation erosion from the axis of symmetry along the longitudinal direction. RDA6 demonstrates autocorrelation in time with a lag of 7 years (r = –0.21, P < 0.01) and a lag of 12 years (r = +0.22, P = 0.02). The variation of the RDA7 axis includes broad– and detailed–scale spatial components, but the broad–scale component is significantly dominated. This axis represents a complex island–like pattern of precipitation erosion variability. RDA7 shows autocorrelation in time with a lag of 3 years (r = 0.24, P = 0.02) and a lag of 13 years (r = –0.25, P = 0.01). The variation of the RDA8 axis includes large–, medium–, and detailed–scale spatial components, but the medium–scale component predominates. This axis also presents a complex island–like pattern of precipitation erosion variability. RDA8 shows autocorrelation in time with a lag of 9 years (r = –0.23, P = 0.01).

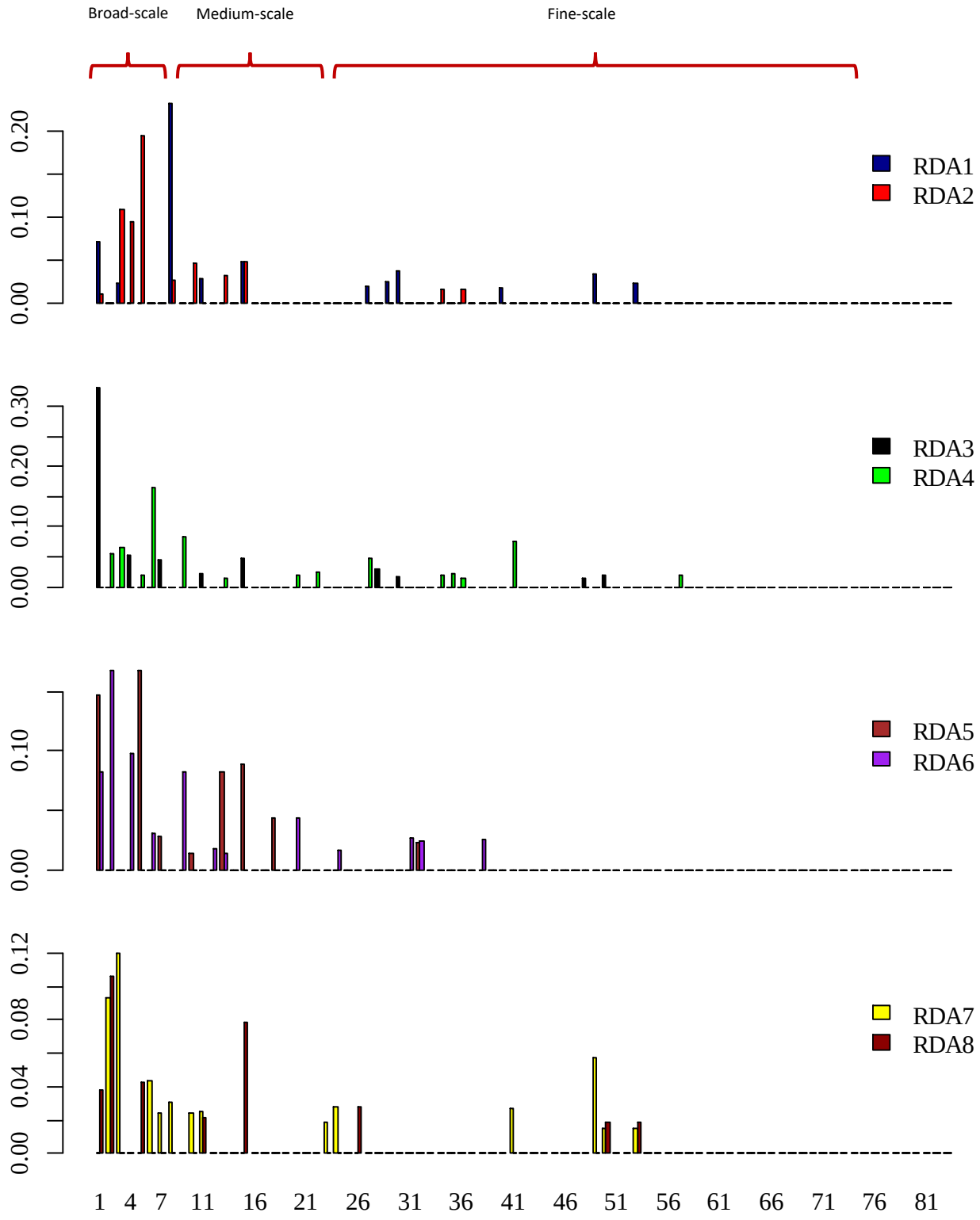

Fig. 2. **Scalogram of the variability of the canonical axes selected after conditional redundancy analysis with spatial MEM variables as predictors. The abscissa axis is the order of spatial MEM variables (1 is the most broadly scaled variable, 83 is the most finely scaled variable). The MEM variables were conditionally grouped into broad–scale (1–10), medium–scale (11–20), and detailed–scale (21–83).**

The role of environmental determinants in the formation of spatial patterns of rainfall erosion

The canonical axes denoting the main spatial patterns of precipitation erosion variability were correlated with soil properties and landscape cover types (Table 1).

1. Correlation between the redundancies identified after conditional analysis with spatial MEM variables as predictors and ecological properties of the territories (correlation coefficients are statistically significant for P < 0.05)

Variables	Canonical variables							
	RDA 1	RDA 2	RDA 3	RDA 4	RDA 5	RDA 6	RDA 7	RDA 8
Soil properties								
Organic matter	–	0.32	–	–0.27	–	–	–0.47	–
Clay	–	–0.73	–	–0.41	–	–0.16	–	–
Sand	–	0.71	–	0.30	–	0.30	–0.14	0.15
Silt	–	–0.60	–	–0.18	–	–0.37	0.19	–0.27
Types of landscape cover (GlobCover)								
Rainfed croplands	0.16	–0.61	–	–0.40	–0.15	–0.19	–	–
Mosaic Croplands	0.47	–0.25	–	–	0.17	–0.23	–	–0.14
Mosaic vegetation	–0.21	–0.35	0.42	–0.26	0.23	–	–	–
Closed broadleaved deciduous forest (> 5m)	–0.37	0.48	–0.14	–	–	0.20	–	–
Closed needleleaved evergreen forest (> 5m)	–	0.33	–	0.47	–	0.15	–	0.17
Open needleleaved deciduous forest (> 5m)	–	0.49	–	0.37	0.18	0.31	–	–
Mixed broadleaved and needleleaved forest (> 5m)	–	0.51	–	0.49	–	0.23	–0.14	0.17
Mosaic grassland	–0.55	–	–	–0.21	–	–	0.29	–
Herbaceous vegetation	–0.41	–	–	–	–	–	0.19	–0.17
Sparse (< 15%) vegetation	0.17	–0.45	–	–0.31	–	–	–	0.16
Grassland or woody vegetation	–	–	–	0.17	–	–	–	–
Artificial surfaces	–	–	–	–	–	–	–	–

The variation in RDA1 was independent of soil properties, but this axis had a negative correlation with the proportion of broadleaf forests and mosaics of herbaceous and shrubs in the landscape cover. This axis had a positive correlation with the proportion of agricultural land. RDA2 was positively correlated with soil organic matter content and sand content, but negatively correlated with clay and silt content in the soil. This axis increased with an increase in the proportion of broadleaf, coniferous, or mixed forests in the landscape cover structure. RDA2 decreased with an increase in the proportion of agricultural crops or sparse vegetation cover. RDA3 did not depend on soil properties. This axis was positively correlated with the proportion of herbaceous and shrub mosaic vegetation and negatively correlated with broadleaf forests. RDA4 was negatively correlated with soil organic matter, clay, and sand content and positively correlated with sand content. This axis decreased with increasing proportions of rainfed crops and a mosaic of herbaceous vegetation and shrubs, but increased with increasing proportions of coniferous, broadleaf, and mixed forests. RDA5 did not correlate with soil properties. This axis increased with increasing proportion of mosaic with crops, but decreased with increasing proportion of coniferous and mixed forests. RDA6 was positively correlated with sand content but negatively correlated with clay and silt content. This axis decreased with increasing proportions of agricultural crops, but increased with increasing proportions of broadleaf, mixed or coniferous forests. RDA7 was positively correlated with silt content but negatively correlated with organic matter and sand content. This axis was positively correlated with the proportion of herbaceous and shrub mosaic vegetation and negatively correlated with the proportion of mixed forests. RDA8 was positively correlated with soil sand content and negatively correlated with silt content. This axis was negatively correlated with the proportion of agricultural land and positively correlated with the proportion of coniferous and mixed forests.

Temporal patterns of precipitation erosion variability for the forecast

The temporal AEM predictors 4, 17, 25, 29, 32, 39, 44, and 61 were able to statistically significantly predict temporal patterns of precipitation variability within the study area (Fig. 3). These temporal predictors were able to explain 25.9% of the variation in the total precipitation erosion coefficient matrix (F = 3.8, P < 0.001). The AEM predictors were able to explain between 13 and 94% of the variability in rainfall erosion within a given administrative region.

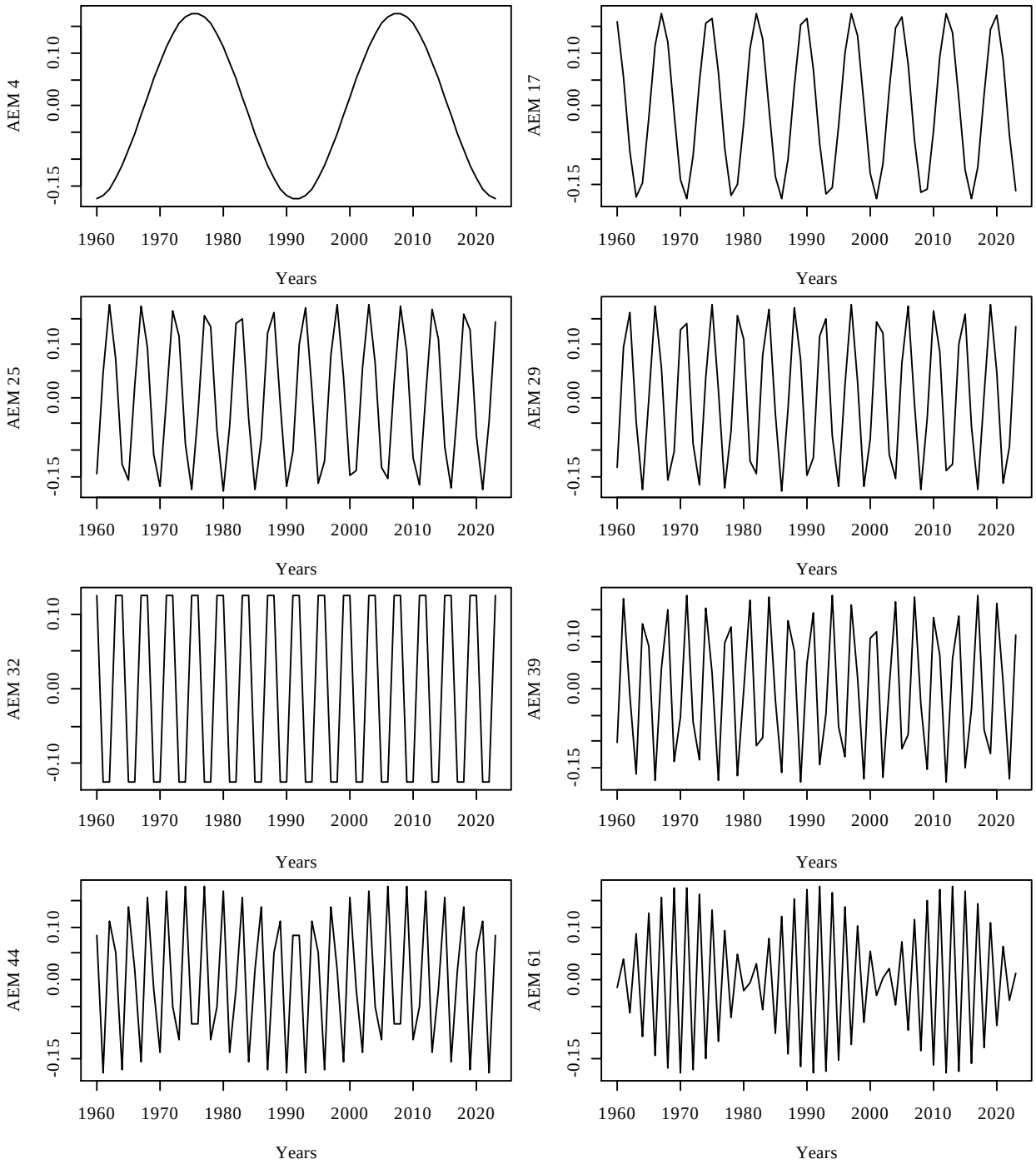

Fig. 3**. AEM-predictors 4, 17, 25, 29, 32, 39, 44 and 61 were able to statistically significantly predict temporal patterns of precipitation variability within the study area**

The highest explanatory power of the AEM predictors was found for the southern and southeastern regions, and the lowest for the western regions (Fig. 4).

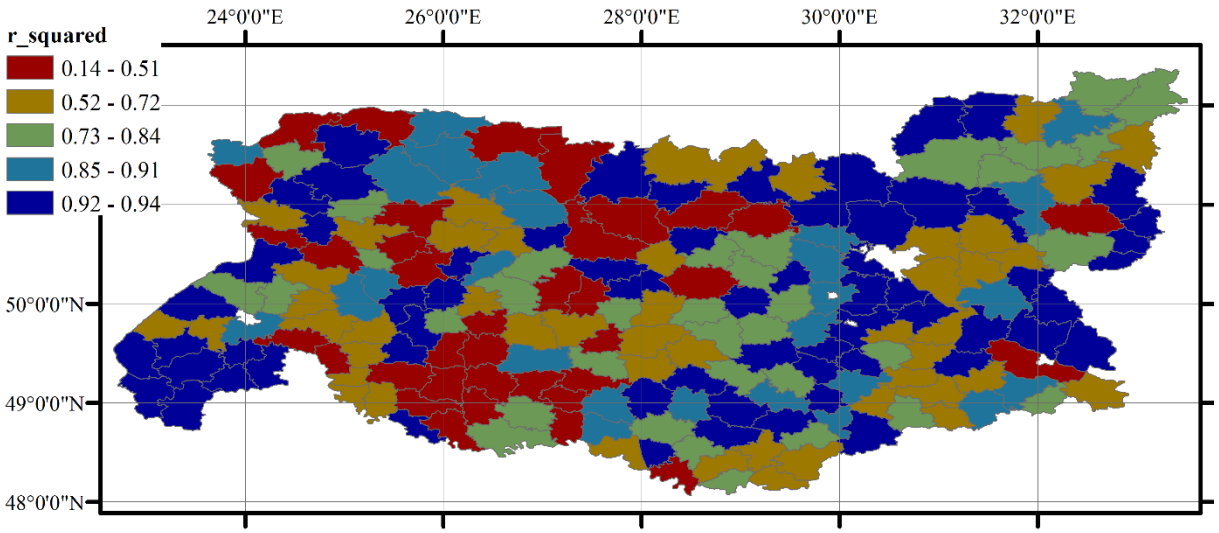

Fig. 4. **Spatial variation of the coefficient of determination of models of rainfall erosion variability with temporal AEM variables as predictors**

The AEM predictors represent regular oscillatory processes, so they can easily be extended into the future, and thus can be used to make a forecast of the dynamics of precipitation erosion in the near future. The forecast for administrative districts was made for the period up to 2060 (Fig. 5). Spatial slices of precipitation variability for demonstration purposes were made for 2040 and 2060 (Fig. 6). In 2040, the zone of minimum precipitation erosion will be located in the central and southeastern parts of the region. In 2060, the overall level of erosion will be lower, and the zone of localized minimum precipitation erosion will be spread throughout the east and center of the region (Fig. 7).

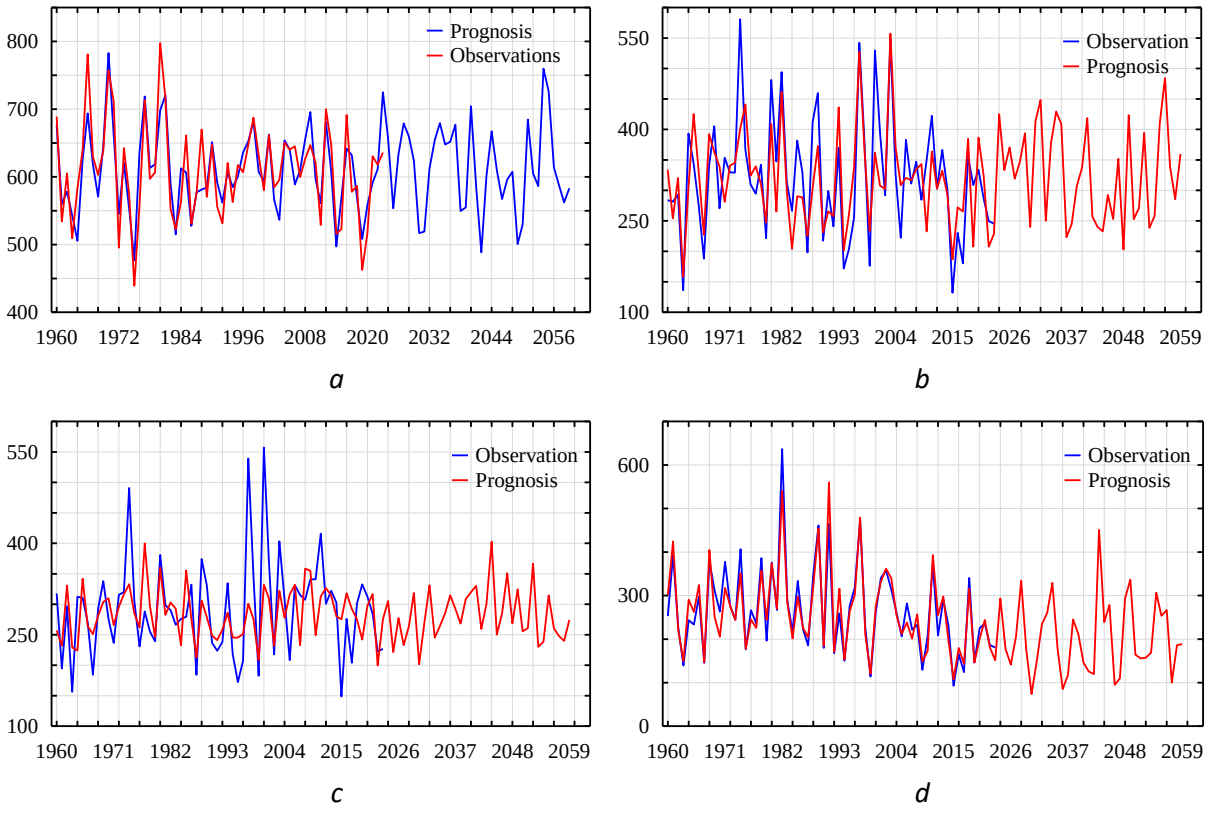

Fig. 5. **Observed amount of precipitation erosion coefficient and estimated precipitation erosion coefficient based on a regression model with time AEM variables as predictors for the period 1960–2023 and forecast to 2060: *a* – Nizhyn district of Chernihiv region; *b* – Bilohirsk district of Khmelnytskyi region; *c* – Dubno district of Rivne region; *d* – Vinnytsia district of Vinnytsia region.**

Discussion

The pattern of precipitation and its amount determine the erosive impact on the soil. The spatial and temporal dynamics of the precipitation erosion factor has a complex hierarchical structure, which can be represented as a set of spatial and temporal patterns with a specific ratio of components at different scales. In the spatial context, the patterns are a superposition of processes of large-, medium-, and detailed-scale levels.

The combination of these levels, the nature of the spatial variability, and the correlation with soil and landscape indicators allows us to formulate hypotheses about the relevant processes that generate spatial patterns of rainfall erosion factors. Obviously, there are three groups of factors that cause natural variability in precipitation erosion. The first group includes factors of geographical nature, the second includes factors caused by soil cover heterogeneity, and the third includes factors caused by landscape cover heterogeneity. The latter also includes factors that are the result of anthropogenic transformation of landscapes, primarily through agricultural activities.

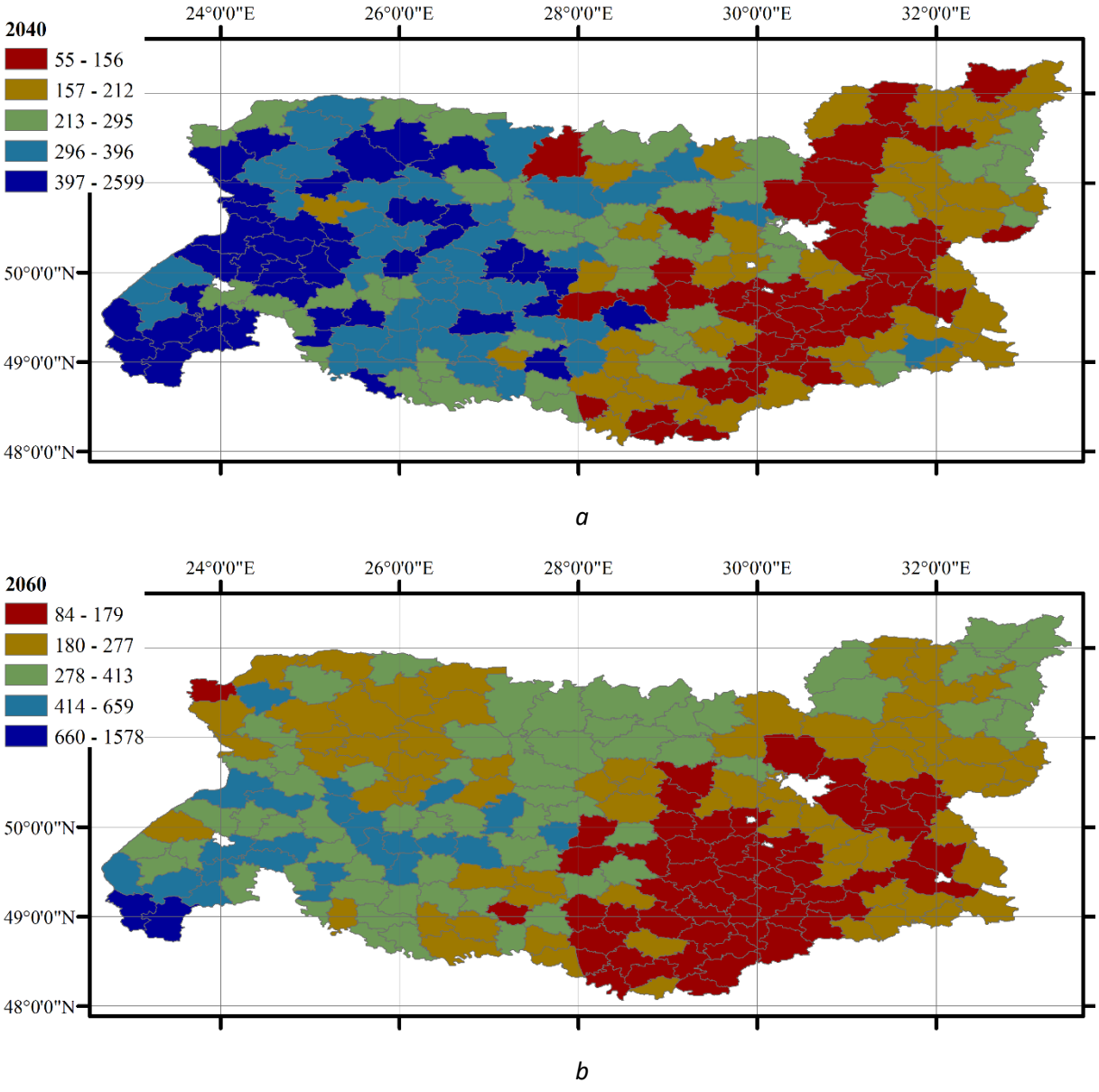

Fig. 6. **Spatial variation of the precipitation erosion coefficient forecast in 2040 (*a*) and 2060 (*b*)**

Geographical origin factors are represented by large-scale patterns, soil factors are represented mainly by medium-scale patterns and to some extent by detailed-scale patterns, and landscape factors are represented mainly by detailed-scale patterns and to a lesser extent by medium-scale patterns. For example, RDA1, 3, 5 do not correlate with soil properties and are mostly represented by large-scale patterns, which indicates that they are generated mainly by factors of geographical origin.

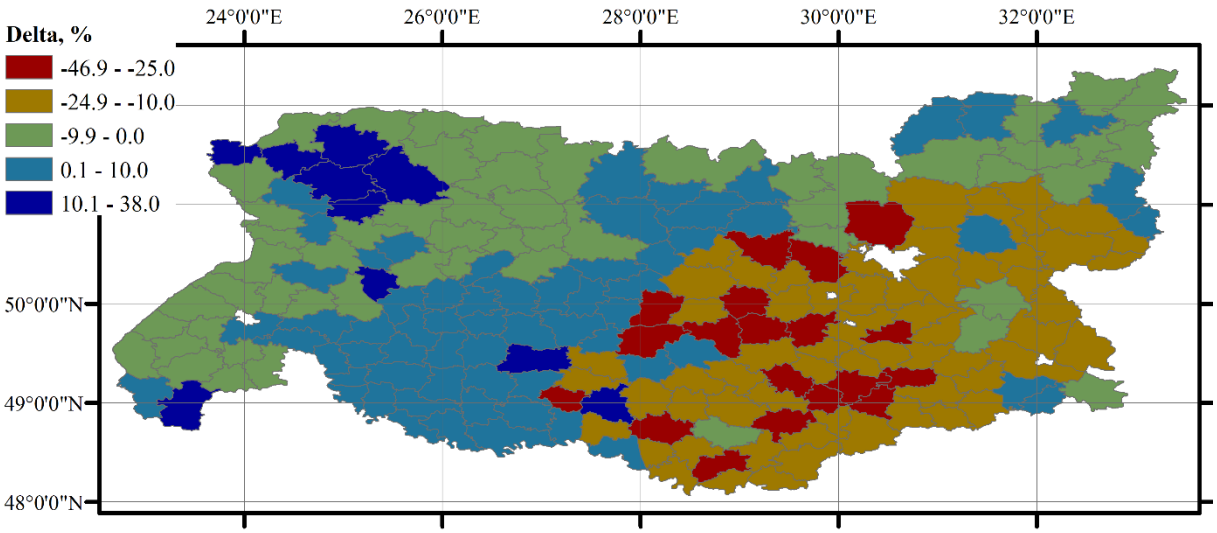

Fig. 7. **Forecast of the spatial variation of the trend of changes in the precipitation erosion coefficient as a % of the average value of the forecast (2024–2060) to the average value of the observed values (1960–2023).**

In fact, RDA1 distinguishes between plains and foothill areas, RDA3 distinguishes between eastern and western zones of the region, which corresponds to meridional zonation, and RDA5 most of all indicates a pattern that can be linked to latitudinal zonation. Geographical variability, including geographical zonation, is a coherent correlation of different natural complexes, including climate, soils, and vegetation. RDA2 is strongly correlated with various soil indicators, and this axis actually distinguishes between the ecological and geographical conditions of Polissya and Forest-Steppe. Geological and geomorphological factors are also involved in the generation of the characteristics of these bioclimatic zones, which is why the soils of Polissya are represented mainly by sandy soils, and the soils of the Forest-Steppe are clay soils.

It should be noted that clay and loamy soils are more favorable for agriculture, so RDA2 is also strongly correlated with the proportion of agricultural soils, which emphasizes the significant difference between the Forest-Steppe, with a much higher proportion of agricultural land, and Polissia, with a much lower proportion. It should be noted, however, that Polissia retains significant areas of coniferous, mixed, and deciduous forests, which is also reflected in the correlation structure of RDA2. The RDA4 axis denotes the central northern zone of the region, where high sand content in the soil is accompanied by lower organic matter and clay and silt content. It should be noted that in other zones of Polissia, the high content of organic matter in the soil is due to its accumulation in bog soils. In the Forest-Steppe, the high content of organic matter in soils is due to the predominance of humification over mineralization and the high ability of soils to immobilize organic matter due to their favorable grain size distribution. The RDA4 axis indicates a zone with a high proportion of coniferous or mixed forests. It should be noted that sandy soils with a low organic matter content have special thermal properties, which directly affects their interaction with the atmosphere,

which affects the processes of evaporation and precipitation. Naturally, changes in the precipitation rhythm cause variability in the precipitation erosion factor.

The temporal predictors indicate a complex temporal nature of the variability of the precipitation erosion factor. It should be noted that the AEM-1 variable indicates a monotonic trend in the change of the corresponding indicator, but this predictor was not statistically significant in explaining the variability of the erosion factor over the study period. Thus, the hypothesis about the directional nature of changes in precipitation and, accordingly, the precipitation erosion factor, due to global climate change, was not confirmed. The dynamics of the erosion factor can be represented as a superposition of oscillatory components of different frequencies and rhythmic changes in amplitude over time. These components have been formally identified, but their meaningful interpretation requires a separate study. Nevertheless, the periodic nature of the temporal predictors of erosion factor variability allows them to be used to predict this indicator in the future.

It should be noted that the forecasting approach has the disadvantage that the forecast estimates somewhat smooth out extreme precipitation forecasts, to which the precipitation erosion factor estimates are very sensitive. The precipitation peaks are well modeled by the regression model, but the forecast values of these peaks are somewhat underestimated. Therefore, the resulting forecasts should be considered to be somewhat conservative, although the general trend of the process is reflected very well by the model results. An important result is that in the near future, a decrease in precipitation erosion can be expected in the southeastern zone of the region, and an increase in precipitation erosion can be expected in the northwestern part of the region.

Conclusion

The spatial and temporal dynamics of the precipitation erosion factor has a complex hierarchical structure, which can be represented as a set of spatial and temporal patterns with a specific ratio of components of large-, medium-, and detailed-scale scale levels. The factors of variability of the precipitation erosion factor of geographical origin are represented by large-scale patterns, soil factors are represented mainly by medium-scale patterns and to some extent by detailed-scale patterns, and landscape factors are represented mainly by detailed-scale patterns and to a lesser extent by medium-scale patterns. The temporal predictors indicate a complex temporal nature of the variability of the precipitation erosion factor. In the short term, a decrease in precipitation erosion can be expected in the southeastern zone of the region within the Forest-Steppe, and an increase in precipitation erosion can be expected in the northwestern part of the region within Polissya.

REFERENCES

Brannigan, N., Mullan, D., Vandaele, K., Graham, C., McKinley, J., & Meneely, J. (2022). Modelling soil erosion by water under future climate change: Addressing methodological gaps. *CATENA*, 216, 106403.

Telo da Gama, J. (2023). The role of soils in sustainability, climate change, and ecosystem services: Challenges and opportunities. *Ecologies,* 4 (3), 552–567.

Horrigan, L., Lawrence, R. S., & Walker, P. (2002). How sustainable agriculture can address the environmental and human health harms of industrial agriculture. *Environmental Health Perspectives*, 110 (5), 445–456.

Panagos, P., Borrelli, P., & Meusburger, K. (2015). A new European slope length and steepness factor (LS-factor) for modeling soil erosion by water. *Geosciences (Switzerland),* 5 (2), 117–126.

Diodato, N., Borrelli, P., Fiener, P., Bellocchi, G., & Romano, N. (2017). Discovering historical rainfall erosivity with a parsimonious approach: A case study in Western Germany. *Journal of Hydrology,* 544, 1–9.

Burt, T., Boardman, J., Foster, I., & Howden, N. (2016). More rain, less soil: long-term changes in

rainfall intensity with climate change. *Earth Surface Processes and Landforms*, 41 (4), 563–566.

Biasutti, M., & Seager, R. (2015). Projected changes in US rainfall erosivity. *Hydrology and Earth System Sciences*, 19 (6), 2945–2961.

Parveen, R., & Kumar, U. (2012). Integrated approach of Universal Soil Loss Equation (USLE) and Geographical Information System (GIS) for soil loss risk assessment in upper south Koel Basin, Jharkhand. *Journal of Geographic Information System,* 04(06), 588–596.

Panagos, P., Ballabio, C., Borrelli, P., Meusburger, K., Klik, A., Rousseva, S., Tadić, M. P., Michaelides, S., Hrabalíková, M., Olsen, P., Aalto, J., Lakatos, M., Rymszewicz, A., Dumitrescu, A., Beguería, S., & Alewell, C. (2015). Rainfall erosivity in Europe. *Science of The Total Environment*, 511, 801–814.

Zymaroieva, A., Zhukov, O., Fedoniuk, T., Pinkina, T., & Vlasiuk, V. (2021). Edaphoclimatic factors determining sunflower yields spatiotemporal dynamics in northern Ukraine. *OCL*, 28 (26), 1–13. https://www.ocl-journal.org/articles/ocl/full_html/2021/01/ocl200109/ocl200109.html

Yin, S., Xie, Y., Liu, B., & Nearing, M. A. (2015). Rainfall erosivity estimation based on rainfall data collected over a range of temporal resolutions. *Hydrology and Earth System Sciences*, 19 (10), 4113–4126.

Panagos, P., Ballabio, C., Borrelli, P., & Meusburger, K. (2016). Spatio-temporal analysis of rainfall erosivity and erosivity density in Greece. *Catena*, 137, 161–172.

Meusburger, K., Steel, A., Panagos, P., Montanarella, L., & Alewell, C. (2012). Spatial and temporal variability of rainfall erosivity factor for Switzerland. *Hydrology and Earth System Sciences*, 16 (1), 167–177.

Diodato, N. (2006). Predicting RUSLE (Revised Universal Soil Loss Equation) Monthly Erosivity Index from Readily Available Rainfall Data in Mediterranean Area. *The Environmentalist*, 26 (1), 63–70.

Václavík, T., Kupfer, J. A., & Meentemeyer, R. K. (2012). Accounting for multi-scale spatial autocorrelation improves performance of invasive species distribution modelling (iSDM). *Journal of Biogeography*, 39 (1), 42–55.

Dray, S., Pélissier, R., Couteron, P., Fortin, M. J., Legendre, P., Peres-Neto, P. R., Bellier, E., Bivand R., Blanchet, F. G., Cáceres, M. De, Dufour, A. B., Heegaard, E., Jombart, T., Munoz, F., Oksanen, J., Thioulouse, J., & Wagner, H. H. (2012). Community ecology in the age of multivariate multiscale spatial analysis. *Ecological Monographs*, 82 (3), 257–275.

Dray, S., Legendre, P., & Peres-Neto, P. R. (2006). Spatial modelling: a comprehensive framework for principal coordinate analysis of neighbour matrices (PCNM). *Ecological Modelling,* 196 (3–4), 483–493.

Borcard, D., & Legendre, P. (2002). All-scale spatial analysis of ecological data by means of principal coordinates of neighbour matrices. *Ecological Modelling,* 153 (1–2), 51–68.

Brind'Amour, A., Mahévas, S., Legendre, P., & Bellanger, L. (2018). Application of Moran Eigenvector Maps (MEM) to irregular sampling designs. *Spatial Statistics*, 26, 56–68.

Ma, X., He, Y., Xu, J., Noordwijk, M. van, & Lu X. (2014). Spatial and temporal variation in rainfall erosivity in a Himalayan watershed. *CATENA*, 121, 248–259.

Wischmeier, W. H., & Smith, D. D. (1978). Predicting rainfall erosion loss: A guide to conservation planning. *Agricultural Handbook.* No. 537. US Department of Agriculture-Agricultural Research Service.

Zerihun, M., Mohammedyasin, M. S., Sewnet, D., Adem, A. A., & Lakew, M. (2018). Assessment of soil erosion using RUSLE, GIS and remote sensing in NW Ethiopia. *Geoderma Regional*, 12, 83–90.

Cedrez, C. B., & Hijmans R. J. (2018). Methods for spatial prediction of crop yield potential. *Agronomy Journal*, 110 (6), 2322–2330.

Fick, S. E., & Hijmans, R. J. (2017). WorldClim 2: new 1-km spatial resolution climate surfaces for global land areas. *International Journal of Climatology*, 37 (12), 4302–4315.

Dray, S., Bauman, D., Blanchet, G., Borcard, D., Clappe, S., Guenard, G., Jombart, T., Larocque, G., Legendre, P., Madi, N., & Wagner, H. H. (2018). adespatial: Multivariate Multiscale Spatial Analysis. R package version 0.3-2. https://CRAN.R-project.org/package=adespatial.

Aksoy, E., Batjes, N., Boateng, E., Fischer, G., Jones, A., Montanarella, L., Shi, X., & Tramberend, S. (2023). Harmonized World Soil Database version 2.0. Ред. Nachtergaele F., Velthuizen H. van, Verelst L. та ін. Rome and Laxenburg:FAO; International Institute for Applied Systems Analysis (IIASA); 1–70 p.

Hijmans, R. J., Barbosa, M., Ghosh, A., & Mandel, A. (2024). Geodata: Download Geographic Data. *R package version 0.6-2*., 2, 1–32.

Одержано редколегією 29.11.2024 р.
Прийнято до друку 18.12.2024 р.